ACS APPLIED MATERIALS & INTERFACES

Research Article

www.acsami.org

Golden Single-Walled Carbon Nanotubes Prepared Using Double Layer Polysaccharides Bridge for Photothermal Therapy

Lingjie Meng,*[,†] Wenjian Xia,[‡,§] Li Liu,[§] Lvye Niu,[‡] and Qinghua Lu*[,‡]

[†]School of Science, Xi'an Jiao Tong University, Xi'an, 710049, P.R. China

[‡]School of Chemistry and Chemical Technology, Shanghai Jiao Tong University, Shanghai, 200240, P. R. China

[§]School of Material Science and Engineering Technology, Shanghai University, Shanghai 201800, P. R. China

Supporting Information

ABSTRACT: Golden single-walled carbon nanotubes (SWNTs) were prepared by growing gold nanoparticles onto the bilayer polysaccharide functionalized SWNTs. The layer-by-layer self-assembly of sodium alginate and chitosan on SWNTs provided an ideal surface with high density of active metal-binding groups such as amino and carboxylic acid groups, and then an approach of seed growth was adopted to facilitate the formation of gold nanoparticles coated SWNTs. The resulting golden SWNT hybrids have good water dispersibility and biocompatibility and tend to enter cancer cells. Interestingly, they have an enhanced NIR absorption and effectively transfer NIR laser into heat. The material can quickly cause localized hyperthermia, resulting in rapid cell death, and therefore appears to act as a highly effective photothermal converter for cancer ablation.

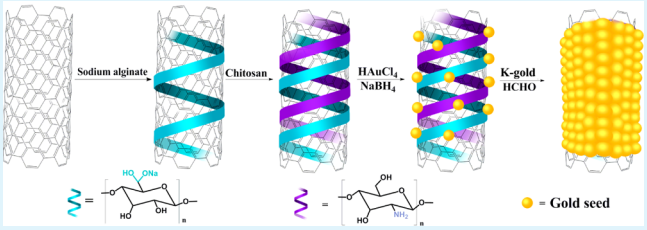

KEYWORDS: *single-walled carbon nanotubes (SWNTs), gold, layer-by-layer, photothermal therapy*

1. INTRODUCTION

Photothermal therapies (PTT) have attracted significant attention in recent years as a promising alternative or supplement to traditional cancer therapies due to their non-invasive and relatively facile implementation.[1−3] The approach focuses on localizing optical absorbing agents at a targeted tissue/organ site, and then irradiating the site with a laser to kill the targeted cells. Because the tissues and blood have low adsorption in the near infrared (NIR) region (650−900 nm),[4,5] the NIR photons are able to penetrate healthy tissues and then be adsorbed selectively in tumors and transformed to heat. Nanostructured materials tend to selectively accumulate in tumor tissues because of their nature of enhanced permeability and retention (EPR) effect.[6,7] Therefore, some nanomaterials with remarkable capacity to absorb light at NIR regions, including gold nanorods,[8,9] gold nanoshells,[10,11] gold nanocages,[12,13] graphene oxide,[14,15] carbon nanotubes,[16,17] and so on, are of great interest for PTT.

Because of their unique physical and chemical properties, carbon nanotubes in general, and single-walled carbon nanotubes (SWNTs) in particular, have generated a lot of interest in nanomedicine for applications in drug delivery, biosensors, tissue engineering, cancer imaging, and thermal therapy.[18−20] However, the SWNTs have a relatively low extinction coefficient (4.4×10^3 $M^{-1}\cdot cm^{-1}$) for PTT while the extinction coefficient of gold nanoparticles is exceptionally high ($\sim1\times10^{19}$ $M^{-1}\cdot cm^{-1}$).[21,22] Recently noble metal nanoparticle coated SWNTs have been found to show an enhanced NIR absorption, improved biocompatibility, excellent photoacoustic and surface enhanced Raman scattering imaging.[23−25] Compared to the frequently-used gold nanorod and nanoshells, these golden SWNTs may act as a unique platform for multimodality disease diagnose and therapy. The pristine SWNTs have insufficient metal-binding groups apart from some carboxyl groups on the defect sites and the tube-ends. To improve the metal loading, suitable modification techniques are generally required to introduce active metal-binding groups (such as amino, carboxylic and thiol groups) onto the SWNT walls.[24,26−29] For example, imidazolium ionic-liquid polymers or poly(sodium 4-styrenesulfonate) has been used to non-covalently functionalize the SWNTs as linkers to immobilize metal nanoparticles.[30−33] However, these ionic polymers are unable to wrap the CNTs densely due to the electrostatic repulsion between the polymer chains, which inevitably make full coverage of metal particles very difficult. As a result, it is still a challenge to develop a facile method to introduce a high density of active metal-binding groups.

In this work, we describe a subtle approach for the synthesis of golden SWNTs nanohybrids by using the layer by layer self-assembly of two oppositely charged polysaccharides (sodium alginate and chitosan) on SWNTs as bridge. In contrast to the conventional methods of single-layer polymer wrapping, this multilayer polysaccharide-wrapping method can result in higher density and more uniform distribution of surface amino and

Received: December 29, 2013
Accepted: March 7, 2014
Published: March 7, 2014

   dx.doi.org/10.1021/am406031n | ACS Appl. Mater. Interfaces 2014, 6, 4989−4996

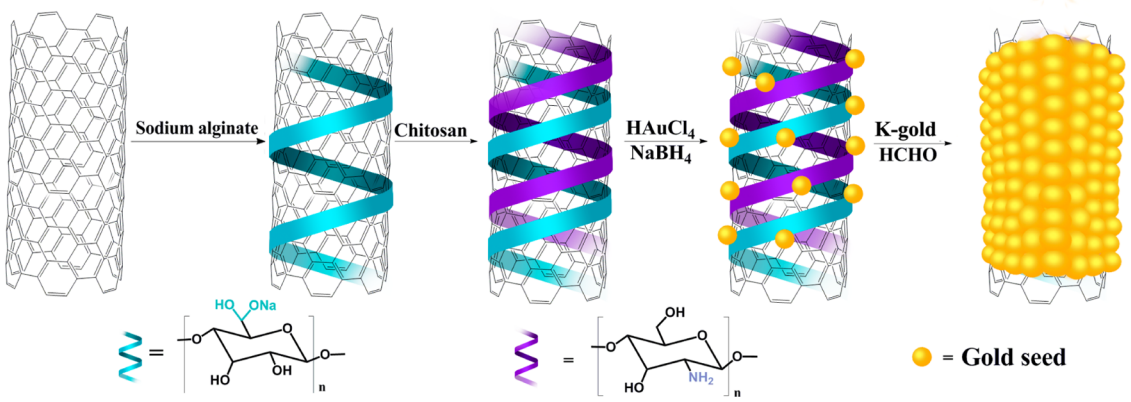

Figure 1. Schematic illustration of the preparation process of golden SWNTs.

carboxylic groups on SWNTs, effectively facilitate the complete decoration of Au nanoparticles. Gold nanoparticles were then deposited on the SWNT surface by an *in situ* reduction approach. As expected, the obtained golden SWNTs have excellent water dispersibility, biocompatibility, and photothermal effect. They also exhibit exceptional effect of photothermal therapy, that is, rapidly leading to tumor cell death.

2. EXPERIMENTAL SECTION

2.1. Chemicals. Raw SWNTs (purity >90%, length ~50 μm, diameter 1-2 nm) were purchased from Chengdu Organic Chemistry Co., Ltd., China. Cut-SWNTs were prepared by cutting and purifying of raw SWNTs following literature methods.[23,34] Sodium alginate (ALG) was purchased from Acros. Chitosan (CHI, 100-300 kDa) was obtained from TCI (Tokyo). Acridine orange (AO) and ethidium bromide (EB) were obtained from Sigma-Aldrich. Fetal bovine serum (FBS) and high glucose Dulbecco's Modified Eagle's medium (DMEM) were purchased from Hyclone. WST-1 cell viability assay kit was purchased from Beyotime Biotechnology Co., Ltd. Chloroauric acid tetrahydrate ($HAuCl_4{\cdot}4H_2O$), sodium borohydride ($NaBH_4$), formaldehyde (37%), and other reagents were purchased from Shanghai Chemical Reagent Co., Ltd. A potassium-basic solution of gold salt (K-gold solution, pH ~10) was prepared by mixing K_2CO_3 with 20 mM $HAuCl_4$ stock solution with continuous stirring in the dark for 12 h. Human cervical carcinoma cells (HeLa) were cultured in high glucose DMEM supplemented with 10% FBS in a humidified incubator (MCO-15AC, Sanyo) at 37 °C (95% room air, 5% CO_2). Porous poly(vinylidene chloride) (PVDC) membrane was purchased from Shanghai ANPEL Instrument Co., Ltd. (50 mm diameter and 0.45 μm pore size). All chemicals were of analytical grade and used as received. Ultra-pure water (18.2 MΩ·cm^{-1}) obtained from a Millipore Milli-Q purification system was used throughout the experiments.

2.2. Preparation of SWNT/ALG/CHI Hybrids. Cut-SWNT suspension (1 mg·mL^{-1}, 30 mL) was added into ALG aqueous solution (2 mg·mL^{-1}, in 0.1 M aqueous NaCl, 30 mL), ultrasonicated for 30 min and stirred vigorously at room temperature for another 24 h. The ALG wrapped SWNTs (SWNT/ALG) were collected by repeated centrifugation (10000 rpm, 10 min) and washing with ultrapure water (5 × 50 mL) to remove the unbound ALG. The as-prepared SWNT/ALG was then ultrasonicated in a CHI solution (2 mg·mL^{-1} in 0.1 M aqueous NaCl and 0.02 M acetic acid, 30 mL) for 30 min. The mixture was vigorously stirred for another 24 h and the product was obtained by following the previous centrifugation and washing procedure. At last, the resultant bilayer polysaccharides wrapped SWNTs (SWNT/ALG/CHI) were obtained and re-suspended into water to make a 0.5 mg·mL^{-1} aqueous solution prior to Au nanoparticles decoration.

2.3. Preparation of Golden SWNTs. Golden SWNTs were prepared in a manner of nucleation and seed growth method. In a typical experiment, $HAuCl_4$ aqueous solution (500 μL, 20 mM) was added in the SWNT/ALG/CHI aqueous solution (10 mL, 0.5 mg·mL^{-1}). $NaBH_4$ aqueous solution (10 mL, 3 mM) was then dropwise added into the mixture under ultrasonic radiation, associated with a color change from light-black to red-purple instantaneously. After ultrasonic irradiation for another 5 min, the reaction mixture was gently stirred at room temperature for 6 h. The resulting SWNT/ALG/CHI/Au seeds were collected by centrifugation (5000 rpm for 10 min), and were further purified twice to remove the free gold nanoparticles by redispersing in 10 mL water and centrifugation. SWNT/ALG/CHI/Au seeds were re-dispersed in water (30 mL) and mixed with K-gold solution (5 mL, 20 mM). The reduction was accomplished by addition of aqueous formaldehyde solution (0.2 mL, 2 wt %) and stirring for another 1 h to generate a blue-purple solution. The resulting golden SWNTs were collected and purified by centrifuging and redispersing in water (50 mL) twice.

2.4. Characterazation. High resolution-transmission electron microscopy (HR-TEM) was conducted on a JEOL TEM-2100 electron microscope (equipped with an energy-dispersive spectrometer, EDS) at 200 kV. Bio-TEM was carried out on a CM120 microscope (Philips). TEM samples were prepared by depositing several drops of dilute solution on a copper micro-grid (230-mesh) and dried at ambient temperature prior to analysis. Field-emission scanning electron microscope (FE-SEM) was carried out on a JEOL JSM-7401F operates at 1 kV. SEM samples were prepared by depositing a drop of dilute solution on clean silicon and drying at 45 °C. XRD patterns were taken by D/max-2200/PC X-ray diffractometer (Rigaku, Japan) in the range of 30−80° (2θ range). Ultraviolet and visible (UV−vis) absorption spectra were recorded on a Lamba 20 spectrometer (Perkin Elmer, Inc.). ζ potentials were measured by a Zeta Potential Analyzer (Zatasizer Nano ZS90, Malvern). Raman spectra were mearsured with a Renishaw in Via Raman microscope using an argon ion laser operating at 514 nm. The photothermal property was conducted by a NIR laser diode (808 nm, 1.6 W, spot size 5×20 mm^2) and digital thermometer (accuracy 0.1 °C), which were purchased from Shenzhen B-Laser Equipment Co., Ltd., China). The viability of HeLa cells cultured with samples was measured in a microplate reader (Bio-Rad, Model 680).

2.5. Photothermal Conversion Experiments. An aqueous suspension of golden SWNTs (2.5 mL, 50 μg·mL^{-1}) was placed in a quartz cell (10 × 10 × 40 mm^3) and exposed to an 808 nm NIR laser source (1.6 W, spot size 5 × 20 mm^2) at a distance of 5 cm. The solution temperature was measured using a HT3500C sensitive thermometer.

2.6. Biocompatibility of Golden SWNTs. HeLa cells were seeded into a 96-well flat culture plate (Corning). After incubation overnight to allow cell attachment, the cells were cultured with golden SWNTs (5, 10, 20, 40, and 50 μg·mL^{-1}, respectively) in a FBS-free culture medium at 37 °C for 24, 48, and 72 h, respectively. They were subsequently rinsed three times with sterilized PBS, and 180 μL PBS was used as a substitute for the culture medium before adding 1:10 (v/v) of the WST-1 reagent (20 μL). After incubation for another 2 h, the

absorbance was measured at 450 nm. Cells cultured without golden SWNTs at the same time intervals were used as controls.

For TEM analysis, HeLa cells were incubated with 20 $\mu g \cdot mL^{-1}$ golden SWNTs for 24 h, and then washed with PBS and fixed with 2% glutaraldehyde and 1% osmium tetroxide for 2 h at 4 °C. The cells were then dehydrated in a graded ethanol series (30%, 50%, 70% with 3% uranyl acetate, 80%, 95%, and 100%) for 10 min at each concentration and followed by two changes in 100% propylene oxide. After infiltration and embedding in epoxy resins at 60 °C for 48 h, the sections were stained with lead citrate and analyzed by Bio-TEM.

2.7. Photothermal Hyperthermia on HeLa Cells. HeLa cells were seeded into a 96-well flat culture plate (Corning). After incubation overnight to allow cell attachment, the cells were incubated with golden SWNTs 50 $\mu g \cdot mL^{-1}$ in a FBS-free culture medium at 37 °C for 24 h. The free golden SWNTs were separated from cultured medium by rinsing three times with PBS. The cells were then irradiated with an 808 nm laser diode (1.6 W, spot size 5 × 20 mm^2) for 15 min. After irradiation, the cell viability was assessed by AO/EB double staining as reported method.[35,36] Stained cells were observed under an inverted fluorescence microscope (IX 71, Olympus) and images were taken using a charge coupled device (CCD, Cascade 650).

3. RESULTS AND DISCUSSION

Preparation of golden SWNTs was a relatively straight forward process (Figure 1). The raw SWNTs were cut and purified

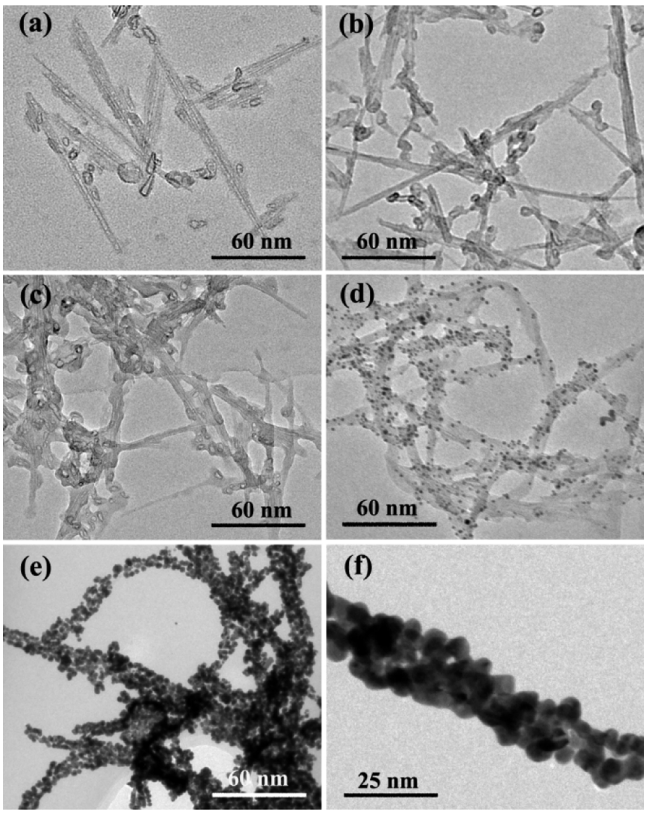

Figure 2. TEM images of (a) cut SWNTs, (b) SWNT/ALG, (c) SWNT/ALG/CHI, (d) SWNT/ALG/CHI/Au seeds, and (e, f) golden SWNTs.

before modification because the raw SWNTs were too long (~50 μm) to enter most of the cells and the motley metal catalysts have been proven to be toxic.[19,34] The defect sites and the tube-ends of cut SWNTs was decorated with carboxyl and hydroxyl groups in the presence of ultrasound and strong oxidizing acids.[37] Therefore, the cut-SWNTs have a good water

Table 1. ζ Potentials of the Modified SWNTs

sample (aqueous solution)	ζ potential (mV, 25 °C)[a]
Cut SWNT	−24.97 ± 0.83
SWNT/ALG	−37.94 ± 1.07
SWNT/CHI	2.56 ± 0.35
SWNT/ALG/CHI	5.83 ± 0.08
SWNT/ALG/CHI/Au seeds	−14.50 ± 0.70
golden SWNTs	−33.40 ± 1.70

[a]Values are averaged from three measurements.

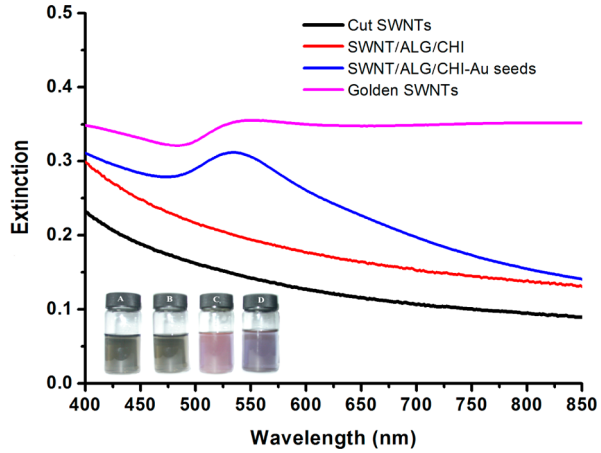

Figure 3. UV−vis spectra of cut SWNTs, SWNT/ALG/CHI, SWNT/ALG/CHI/Au seeds, and golden SWNTs. Inset: Photographs of cut SWNTs (A), SWNT/ALG/CHI (B), SWNT/ALG/CHI/Au seeds (C), and golden SWNTs (D) aqueous solutions.

dispersibility due to their hydrophilic groups and electrostatic interactions, which provide a favorable condition for the modification by polysaccharides. The encapsulation of SWNTs by the polysaccharides was achieved in a two-step process involving initial treatment with ALG followed by CHI. The Au nanoparticles were then formed on the SWNT/ALG/CHI by *in situ* reduction of $HAuCl_4$ to generate SWNT/ALG/CHI-Au seeds. The golden SWNTs were finally obtained in a manner of seed-mediated growth and the golden SWNT solution showed a characteristic blue color owing to the SPR absorption of the coated gold nanoparticles.[23,24,38]

The structures and morphologies of the modified SWNTs were studied by HR-TEM and FE-SEM. Purified SWNTs have smooth and inert graphite sidewalls with only few carboxyl and hydroxyl groups on the defect sites,[37] and tend to form bundles that dispersed poorly in aqueous solution (see Figure S1, Supporting Information). After cutting in the mixture of concentrated HNO_3 and H_2SO_4 under ultrasonication, the cut SWNTs are generally short (< 500 nm) and well separated (Figure 2a). In our previous research, natural polysaccharides can be helically wrapped onto the SWNT walls via hydrophobic force and hydrogen bond.[39,40] However, only sparse CHI and ALG molecular chains can be observed on the sidewalls of SWNTs (see Figure 2b and Figure S2a, Supporting Information). To further introduce more metal-binding groups on the SWNT surface, a two-step process involving initial treatment with negatively-charged ALG followed by positively-charged CHI was carried out, leading to the double-layer encapsulation of both CHI and ALG on the SWNT core by electrostatic assembly. As expected, the double layered polysaccharides present in SWNT/ALG/CHI are obviously

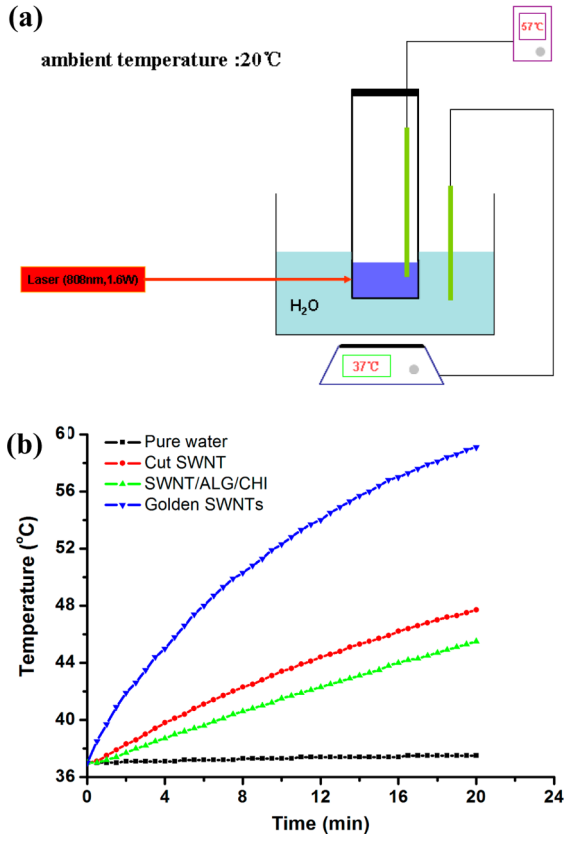

Figure 4. (a) Schematic simulation for photothermal conversion of golden SWNTs solution exposed by a NIR laser and (b) the photothermal curves of modified SWNTs (50 $\mu g \cdot mL^{-1}$) irradiated with an 808 nm laser.

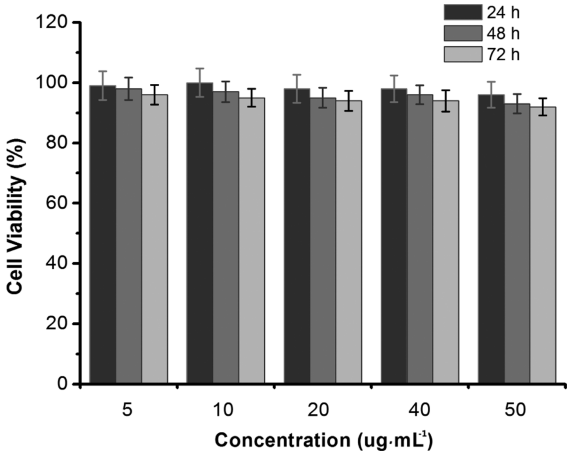

Figure 5. Cell viability of HeLa cells after incubating with golden SWNTs at various concentrations (5, 10, 20, 40, 50 $\mu g \cdot mL^{-1}$) for 24, 48, and 72 h, respectively.

thicker than the coating in SWNT/ALG and SWNT/CHI (Figure 2c). When the $HAuCl_4$ aqueous solution was reduced quickly by a strong reducing agent ($NaBH_4$), instantaneous Au atoms were bound to the surface of SWNT/ALG/CHI, to which more atoms would be adsorbed to form several relatively small (*ca.* 2-4 nm) Au particles (Figure 2d). Further reducing additional gold salt by a slow reduction procedure using a relatively mild reducer (formaldehyde, CH_2O), more Au nanoparticles deposited on the amino and carboxyl sites and the Au seeds on the SWNT/ALG/CHI also continued to grow up. Eventually, Au nanoparticles completely coated on the SWNTs to form golden SWNTs (Figure 2e and f). In contrast, SWNT/CHI/Au hybrids were prepared using the same procedure (see Figure S2, Supporting Information). The Au nanoparticles cannot fully cover the SWNT/CHI because CHI chains were wrapping on the SWNTs incompletely, leading to insufficient metal-binding sites on the SWNTs. Therefore, this multilayer polysaccharide-assembly method is necessary for the formation of complete gold shells on SWNTs. The morphologies of cut SWNTs, SWNT/ALG, SWNT/ALG/CHI, SWNT/ALG/CHI/Au seeds and golden SWNTs were characterized by FE-SEM (see Figure S3, Supporting Information). The length and diameter of these carbon nanotubes from SEM are consistent with that of TEM. And, the golden SWNTs have a very rough surface that should benefit surface modification and light absorption.

ζ-Potential measurements further demonstrated the coating process of polysaccharides and Au nanoparticles onto SWNTs (Table 1). The surface potential of the cut SWNTs is -24.97 ± 0.83 mV because of the ionization of surface carboxyl acid groups. After functionalized by positively charged CHI or negatively charged ALG, the potential of SWNT/CHI accordingly increased to 2.56 ± 0.35 mV while that of SWNT/ALG decreased to -37.94 ± 1.07 mV. As expected, the potential of SWNT/ALG/CHI has obviously increased by 43.8 mV compared with that of SWNT-ALG, which confirms the consecutive wrapping of ALG and CHI on SWNT surface through layer-by-layer electrostatic wrapping manner. Interestingly, the potential increase of SWNT/ALG/CHI versus SWNT/ALG (43.8 mV) is larger than that of SWNT-CHI versus SWNTs (26.0 mV), suggesting that the intermediate negatively-charged ALG layer could play an important role to increase the electroadsorption of positively charged CHI. After further growing the negatively charged Au nanoparticles onto the SWNT/ALG/CHI, the potentials of SWNT/ALG/CHI/Au seeds and golden SWNTs reduced to -14.50 ± 0.70 and -33.40 ± 1.70 mV, respectively.

EDS and XRD analysis was also carried out to study the formation of the golden SWNTs. Signals for Au (M_α and L_α at 2.12 and 9.71 keV, respectively) were observed in the EDS spectrum of golden SWNTs (see Figure S4, Supporting Information), indicating the presence of Au on the SWNTs. The other elements such as oxygen and carbon should come from polysaccharides and carbon nanotubes (copper excluded, caused by copper mesh). The crystallinity of gold nanoparticles on SWNTs was further characterized by XRD diffraction spectrum (see Figure S5, Supporting Information). Au nanoparticles on SWNTs exhibited a good crystallinity and the regular lattice diffraction peaks (2θ) at 38.18°, 44.39°, 64.58°, 77.55°, and 81.72° should be corresponding to the crystal plane (111), (200), (220), (311), and (222) of Au, exhibiting a typical face-centered cubic structure. It was noted that the intensity of diffraction peaks was obviously enhanced from SWNT/ALG/CHI/Au seeds to golden SWNTs, demonstrating that the initial small Au nanoparticles were grown up by the manner of seed growth.

Interactions between polysaccharides, gold nanoparticles and SWNTs were investigated by Raman spectra (see Figure S6, Supporting Information). The Raman spectra have three main characteristic peaks, including D band (~1350 cm^{-1}), resulting from amorphous carbon and the disorder graphite structure (defects), and the G and 2D band (~1590 and 2600 cm^{-1},

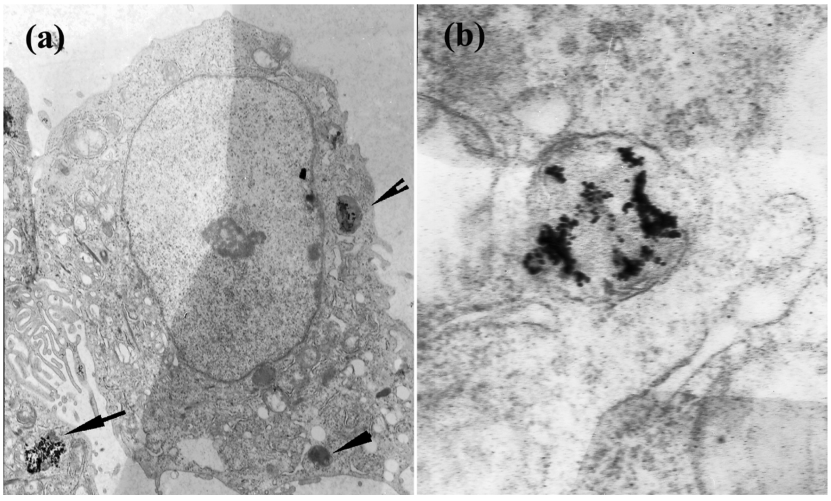

Figure 6. TEM images of (a) HeLa cells cultured with the golden SWNTs (20 $\mu g \cdot mL^{-1}$) for 24 h, the black arrows point to internalized golden SWNTs, and (b) magnified region of a lysosome .

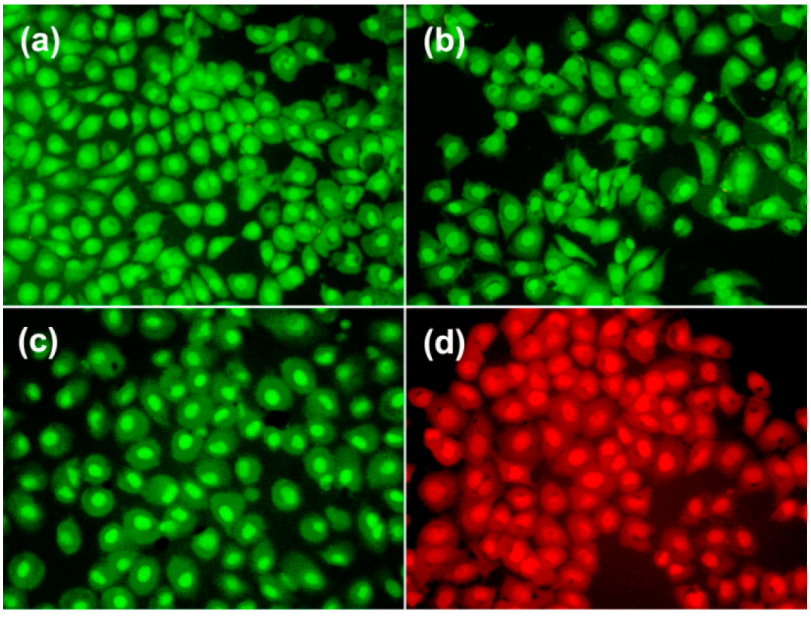

Figure 7. Fluorescence microscopy images of (a) Hela cells, (b) HeLa cells incubated with golden SWNTs (50 $\mu g \cdot mL^{-1}$) for 24 h (c) HeLa cells subjected to NIR irradiation for 15 min, and (d) HeLa cells incubated with golden SWNTs (50 $\mu g \cdot mL^{-1}$) for 24 h (in the dark) and then subjected to NIR irradiation. The cells were stained by AO and EB.

respectively) which reflect the structure of the sp^2-hybridized carbon atoms in highly crystalline graphite.[41,42] The extent of the defects in SWNTs were generally evaluated by the intensity ratio of the D and G bands (i.e., I_D/I_G).[43] The values of the I_D/I_G ratio for the pristine SWNT, cut SWNT, SWNT/ALG/CHI and golden SWNTs were 0.07, 0.26, 0.28, and 0.29, respectively. The I_D/I_G value of cut SWNT (0.26) was obviously higher than that of the pristine SWNTs (0.07), indicating that the sp^2 structure of cut SWNTs was severely damaged during treating by the long-time sonication and harsh acid treatment. In comparison, there were no obvious I_D/I_G changes after being further coated by polysaccharides and gold nanoparticles. It suggested that the coating of polysaccharides and gold nanoparticles would not cause the sp^2 structural damage of SWNTs. The golden SWNTs and SWNT/ALG/CHI have similar Raman spectra compared to that of the cut SWNTs except a slight G and 2D peak shift because the G and 2D peaks are very sensitive to the environment.[44] The G and 2D peaks of cut SWNTs were 1581 and 2672 cm^{-1}, but that of SWNT/ALG/CHI and golden SWNTs shift to (1589, 2683 cm^{-1}) and (1596, 2687 cm^{-1}), respectively, indicating the interactions between polysaccharides, gold nanoparticles and SWNTs.

The UV−vis spectra were recorded to examine the absorption profile of the SWNTs species (Figure 3). The aqueous solution of cut SWNT and SWNT/ALG/CHI are typically grey, and they have no noticeable absorption peak between 400−850 nm. Whereas the SWNT/ALG/CHI/Au seed solution shows a purple color and has a characteristic peak at about 530 nm which should be attributed to the surface plasmon resonances (SPR) of single gold nanoparticles on the SWNT/ALG/CHI.[45,46] With the depositing of gold nanoparticles, the aqueous solution gradually turned from purple to blue, indicating that gold nanoparticles have completely

covered the SWNTs. The golden SWNTs showed a strong plasmon resonance absorption between 550 and 850 nm due to the photoelectric fields polarize along the long axis of SWNTs. In contrast, the SWNT/CHI/Au hybrids did not have strong absorption in the NIR region except the characteristic peak of Au nanoparticles at about 530 nm (see Figure S7, Supporting Information). Therefore, the golden SWNTs is a kind of brand new nano-hybrid with great NIR absorption and thereby might efficiently transform the absorbed NIR light-energy into heat.

The photothermal conversion of the golden SWNTs was further studied using an 808 nm semiconductor laser at the simulating human body temperatures, with pure water, cut SWNTs and SWNT/ALG/CHI suspensions used as controls. The quartz cuvette with SWNT aqueous solution was placed into a 37 °C bath and irradiated by an 808 nm laser, and a thermocouple digital thermometer was used to monitor the solution temperature change (Figure 4a). All the suspensions of SWNT samples resulted in obvious heating after exposure for 20 min, whereas pure water always kept at 37 °C without any absorption (Figure 4b). Though carbon nanotubes have a relatively low absorption in the NIR region, they were still used as the thermal-ablation agents due to their excellent thermal conductivity and specific nano-effects.[16,17,47] The absorption of SWNT/ALG/CHI (from 400 to 850 nm) is lower than that of cut SWNTs at the same concentration, probably because the polysaccharide layer have no absorption in this range and might decrease the thermal conductivity of SWNTs. As a result, the photothermal property of SWNT/ALG/CHI is a slightly less efficient than that of cut SWNTs. Interestingly, the suspension of golden SWNTs is heating up at nearly twice the rate of cut SWNTs, approaching 57 °C after 20 min exposure that is high enough to kill tumor cells.[23,38] Thereby, the golden SWNTs have the highest photothermal efficiency and have great potential for PTT.

We quantitatively assessed the cytotoxicity of golden SWNTs by WST-1 assay because the safety of any nanomaterials is of utmost importance when considering their biomedical applications. The golden SWNTs showed no appreciable cytotoxicity when incubating with HeLa cells in the concentration range of 5−50 ug·mL^{-1} for 24, 48, and 72 h (Figure 5). Though there have been many conflicting data about the toxicity of carbon nanotubes,[18,20] the HeLa cells exhibit a high tolerance to golden SWNTs probably because the polysaccharide layer and Au nanoparticles are biocompatible.

TEM images further gave the unequivocal evidences of golden SWNT biodistribution in HeLa cells (Figure 6). The golden SWNTs were internalized by HeLa cells and mainly located at some cellular vesicles such as lysosomes. The accumulation of golden SWNTs in cells is good for the photothermal conversion to kill the tumor cells.

The photothermal effects in vitro were investigated by a AO/EB double staining assay (Figure 7).[24,37] Healthy cells typically have green nuclei and uniform chromatin with an intact cell membrane, whereas cells in necrosis or late stages of apoptosis have red nuclei. After they were cultured for 24 h, all the HeLa cells incubated with golden SWNTs (50 μg·mL^{-1}) or irritated under a 808 nm laser alone for 15 min remain healthy with green nuclei (Figure 7b and c), suggesting that neither golden SWNTs or 808 nm laser alone are harmful for cells. Whereas, if the HeLa cells are cultured with golden SWNTs (50 μg·mL^{-1}) for 24 h and followed by NIR irradiation for 15 min, all the HeLa cells are already in necrosis, with the nuclei turning red (Figure 7d). On the basis of the results of Figures 6 and 7, it is reasonable to suppose that the golden SWNTs tend to enter and locate in the HeLa cells by membrane-penetration or cell endocytosis, and then absorb NIR laser and convert into heat. This sudden temperature increase triggered the death of the HeLa cells.

4. CONCLUSIONS

In conclusion, we have developed a facile method to prepare gold nanoparticles coated SWNTs (golden SWNTs) by seed growth of gold nanoparticles on the bilayer polysaccharides functionalized SWNTs. The layer-by-layer self-assembly of two polysaccharides with opposite charge (that is, ALG and CHI) provided an ideal surface with high density of active metal-binding groups such as amino and carboxylic acid groups for further generating golden SWNTs. Golden SWNT hybrids have good water dispersibility and biocompatibility, and tend to enter cancer cells and locate in lysosomes. Interestingly, they have an enhanced NIR absorption that is effectively transferred NIR laser into heat. The material can quickly cause localized hyperthermia, resulting in rapid tumor cell death, and therefore appears to act as a highly effective photothermal converter for cancer ablation.

■ ASSOCIATED CONTENT

Ⓢ Supporting Information

TEM image of purified SWNTs, photographs of the aqueous solutions of purified SWNTs and cut SWNTs, TEM images of SWNT/CHI/Au hybrids, FE-SEM images of modified SWNTs, EDX spectrum of golden SWNTs, XRD spectra of SWNT-ALG/CHI-Au seeds and golden SWNTs, Raman spectra of modified SWNTs, and UV−vis absorption spectra of SWNT/CHI/Au hybrids. This material is available free of charge via the Internet at http://pubs.acs.org.

■ AUTHOR INFORMATION

Corresponding Authors

*E-mail: menglingjie@mail.sjtu.edu.cn.
*Fax: 86-21-54747535. E-mail: qhlu@sjtu.edu.cn.

Notes

The authors declare no competing financial interest.

■ ACKNOWLEDGMENTS

This work was supported by National Science Foundation for Distinguished Young Scholars (50925310), the National Science Foundation of China (20904030, 21174087), Major Project of Chinese National Programs for Fundamental Research and Development (973 Project: 2009CB930400), China Postdoctoral Science Foundation (18420011) and the Fundamental Funds for the Central Universities (DWHXC101000074).

■ REFERENCES

(1) O'Neal, D. P.; Hirsch, L. R.; Halas, N. J.; Payne, J. D.; West, J. L. Photo-Thermal Tumor Ablation in Mice Using near Infrared-Absorbing Nanoparticles. *Cancer Lett.* **2004**, *209*, 171−176.

(2) Gobin, A. M.; Lee, M. H.; Halas, N. J.; James, W. D.; Drezek, R. A.; West, J. L. Near-Infrared Resonant Nanoshells for Combined Optical Imaging and Photothermal Cancer Therapy. *Nano Lett.* **2007**, *7*, 1929−1934.

(3) Jain, P. K.; Huang, X.; El-Sayed, I. H.; El-Sayed, M. A. Noble Metals on the Nanoscale: Optical and Photothermal Properties and Some Applications in Imaging, Sensing, Biology, and Medicine. *Acc. Chem. Res.* **2008**, *41*, 1578−1586.

(4) Huang, X. H.; El-Sayed, I. H.; Qian, W.; El-Sayed, M. A. Cancer Cell Imaging and Photothermal Therapy in the Near-Infrared Region by Using Gold Nanorods. *J. Am. Chem. Soc.* **2006**, *128*, 2115−2120.
(5) Huang, C.-C.; Su, C.-H.; Li, W.-M.; Liu, T.-Y.; Chen, J.-H.; Yeh, C.-S. Bifunctional Gd_2O_3/C Nanoshells for MR Imaging and NIR Therapeutic Applications. *Adv. Funct. Mater.* **2009**, *19*, 249−258.
(6) Gao, X. H.; Cui, Y. Y.; Levenson, R. M.; Chung, L. W. K.; Nie, S. M. In Vivo Cancer Targeting and Imaging with Semiconductor Quantum Dots. *Nat. Biotechnol.* **2004**, *22*, 969−976.
(7) Jain, R. K.; Stylianopoulos, T. Delivering Nanomedicine to Solid Tumors. *Nat. Rev. Clin. Oncol.* **2010**, *7*, 653−664.
(8) Dickerson, E. B.; Dreaden, E. C.; Huang, X.; El-Sayed, I. H.; Chu, H.; Pushpanketh, S.; McDonald, J. F.; El-Sayed, M. A. Gold Nanorod Assisted Near-Infrared Plasmonic Photothermal Therapy (PPTT) of Squamous Cell Carcinoma in Mice. *Cancer Lett.* **2008**, *269*, 57−66.
(9) Tong, L.; Wei, Q.; Wei, A.; Cheng, J.-X. Gold Nanorods as Contrast Agents for Biological Imaging: Optical Properties, Surface Conjugation and Photothermal Effects. *Photochem. Photobiol.* **2009**, *85*, 21−32.
(10) Bardhan, R.; Lal, S.; Joshi, A.; Halas, N. J. Theranostic Nanoshells: From Probe Design to Imaging and Treatment of Cancer. *Acc. Chem. Res.* **2011**, *44*, 936−946.
(11) Ke, H.; Wang, J.; Dai, Z.; Jin, Y.; Qu, E.; Xing, Z.; Guo, C.; Yue, X.; Liu, J. Gold-Nanoshelled Microcapsules: A Theranostic Agent for Ultrasound Contrast Imaging and Photothermal Therapy. *Angew. Chem. Int. Ed.* **2011**, *50*, 3017−3021.
(12) Gao, L.; Fei, J.; Zhao, J.; Li, H.; Cui, Y.; Li, J. Hypocrellin-Loaded Gold Nanocages with High Two-Photon Efficiency for Photothermal/Photodynamic Cancer Therapy in Vitro. *ACS Nano* **2012**, *6*, 8030−8040.
(13) Yavuz, M. S.; Cheng, Y.; Chen, J.; Cobley, C. M.; Zhang, Q.; Rycenga, M.; Xie, J.; Kim, C.; Song, K. H.; Schwartz, A. G.; Wang, L. V.; Xia, Y. Gold Nanocages Covered by Smart Polymers for Controlled Release with Near-Infrared Light. *Nat. Mater.* **2009**, *8*, 935−939.
(14) Yang, K.; Zhang, S.; Zhang, G.; Sun, X.; Lee, S.-T.; Liu, Z. Graphene in Mice: Ultrahigh in Vivo Tumor Uptake and Efficient Photothermal Therapy. *Nano Lett.* **2010**, *10*, 3318−3323.
(15) Robinson, J. T.; Tabakman, S. M.; Liang, Y.; Wang, H.; Casalongue, H. S.; Daniel, V.; Dai, H. Ultrasmall Reduced Graphene Oxide with High Near-Infrared Absorbance for Photothermal Therapy. *J. Am. Chem. Soc.* **2011**, *133*, 6825−6831.
(16) Moon, H. K.; Lee, S. H.; Choi, H. C. In Vivo Near-Infrared Mediated Tumor Destruction by Photothermal Effect of Carbon Nanotubes. *ACS Nano* **2009**, *3*, 3707−3713.
(17) Zhou, F.; Xing, D.; Ou, Z.; Wu, B.; Resasco, D. E.; Chen, W. R. Cancer Photothermal Therapy in the near-Infrared Region by Using Single-Walled Carbon Nanotubes. *J. Biomed. Opt.* **2009**, *14*, 021009.
(18) Liu, Z.; Tabakman, S.; Welsher, K.; Dai, H. Carbon Nanotubes in Biology and Medicine: In Vitro and in Vivo Detection, Imaging and Drug Delivery. *Nano Res.* **2009**, *2*, 85−120.
(19) Meng, L.; Zhang, X.; Lu, Q.; Fei, Z.; Dyson, P. J. Single Walled Carbon Nanotubes as Drug Delivery Vehicles: Targeting Doxorubicin to Tumors. *Biomaterials* **2012**, *33*, 1689−1698.
(20) Kostarelos, K.; Bianco, A.; Prato, M. Promises, Facts and Challenges for Carbon Nanotubes in Imaging and Therapeutics. *Nat. Nanotechnol.* **2009**, *4*, 627−633.
(21) Schoeppler, F.; Mann, C.; Hain, T. C.; Neubauer, F. M.; Privitera, G.; Bonaccorso, F.; Chu, D.; Ferrari, A. C.; Hertel, T. Molar Extinction Coefficient of Single-Wall Carbon Nanotubes. *J. Phys. Chem. C* **2011**, *115*, 14682−14686.
(22) Link, S.; El-Sayed, M. A. Shape and Size Dependence of Radiative, Non-Radiative and Photothermal Properties of Gold Nanocrystals. *Int. Rev. Phys. Chem.* **2000**, *19*, 409−453.
(23) Meng, L.; Niu, L.; Li, L.; Lu, Q.; Fei, Z.; Dyson, P. J. Gold Nanoparticles Grown on Ionic Liquid-Functionalized Single-Walled Carbon Nanotubes: New Materials for Photothermal Therapy. *Chem.—Eur. J.* **2012**, *18*, 13314−13319.
(24) Wang, X.; Wang, C.; Cheng, L.; Lee, S.-T.; Liu, Z. Noble Metal Coated Single-Walled Carbon Nanotubes for Applications in Surface Enhanced Raman Scattering Imaging and Photothermal Therapy. *J. Am. Chem. Soc.* **2012**, *134*, 7414−7422.
(25) Kim, J.-W.; Galanzha, E. I.; Shashkov, E. V.; Moon, H.-M.; Zharov, V. P. Golden Carbon Nanotubes as Multimodal Photoacoustic and Photothermal High-Contrast Molecular Agents. *Nat. Nanotechnol.* **2009**, *4*, 688−694.
(26) Segura del Rio, R. Non-Covalent Assembly of Hybrid Nanostructures of Gold and Palladium Nanoparticles with Carbon Nanotubes. *Int. J. Mater. Res.* **2012**, *103*, 901−905.
(27) Kim, Y. S.; Cha, A.; Shin, J. Y.; Jeon, H. J.; Shim, J. H.; Lee, C.; Lee, S.-g. High-Density Assembly of Gold Nanoparticles with Zwitterionic Carbon Nanotubes and Their Electrocatalytic Activity in Oxygen Reduction Reaction. *Chem. Commun.* **2012**, *48*, 8940−8942.
(28) Wu, B.; Hu, D.; Kuang, Y.; Liu, B.; Zhang, X.; Chen, J. Functionalization of Carbon Nanotubes by an Ionic-Liquid Polymer: Dispersion of Pt and PtRu Nanoparticles on Carbon Nanotubes and Their Electrocatalytic Oxidation of Methanol. *Angew. Chem., Int. Ed.* **2009**, *48*, 4751−4754.
(29) Yang, W.; Wang, Y.; Li, J.; Yang, X. Polymer Wrapping Technique: An Effective Route to Prepare Pt Nanoflower/Carbon Nanotube Hybrids and Application in Oxygen Reduction. *Energy Environ. Sci.* **2010**, *3*, 144−149.
(30) Dykman, L.; Khlebtsov, N. Gold Nanoparticles in Biomedical Applications: Recent Advances and Perspectives. *Chem. Soc. Rev.* **2012**, *41*, 2256−2282.
(31) Xi, D.; Dong, S.; Meng, X.; Lu, Q.; Meng, L.; Ye, J. Gold Nanoparticles as Computerized Tomography (CT) Contrast Agents. *RSC Adv.* **2012**, *2*, 12515−12524.
(32) Mieszawska, A. J.; Mulder, W. J. M.; Fayad, Z. A.; Cormode, D. P. Multifunctional Gold Nanoparticles for Diagnosis and Therapy of Disease. *Mol. Pharmacol.* **2013**, *10*, 831−847.
(33) Dobbins, T.; Chevious, R.; Lvov, Y. Behavior of Na^+-Polystyrene Sulfonate at the Interface with Single-Walled Carbon Nanotubes (SWNTS) and Its Implication to SWNT Suspension Stability. *Polymers* **2011**, *3*, 942−954.
(34) Zhang, X.; Meng, L.; Lu, Q.; Fei, Z.; Dyson, P. J. Targeted Delivery and Controlled Release of Doxorubicin to Cancer Cells Using Modified Single Wall Carbon Nanotubes. *Biomaterials* **2009**, *30*, 6041−6047.
(35) Li, L.; Meng, L. J.; Zhang, X. K.; Fu, C. L.; Lu, Q. H. The Ionic Liquid-Associated Synthesis of a Cellulose/SWCNT Complex and Its Remarkable Biocompatibility. *J. Mater. Chem.* **2009**, *19*, 3612−3617.
(36) Zhou, J. F.; Meng, L. J.; Feng, X. L.; Zhang, X. K.; Lu, Q. H. One-Pot Synthesis of Highly Magnetically Sensitive Nanochains Coated with a Highly Cross-Linked and Biocompatible Polymer. *Angew. Chem. Int. Ed.* **2010**, *49*, 8476−8479.
(37) Zhang, J.; Zou, H. L.; Qing, Q.; Yang, Y. L.; Li, Q. W.; Liu, Z. F.; Guo, X. Y.; Du, Z. L. Effect of Chemical Oxidation on the Structure of Single-Walled Carbon Nanotubes. *J. Phys. Chem. B* **2003**, *107*, 3712−3718.
(38) Zhou, J.; Meng, L.; Lu, Q. Core@Shell Nanostructures for Photothermal Conversion: Tunable Noble Metal Nanoshells on Cross-Linked Polymer Submicrospheres. *J. Mater. Chem.* **2010**, *20*, 5493−5498.
(39) Zhang, X.; Meng, L.; Lu, Q. Cell Behaviors on Polysaccharide-Wrapped Single-Wall Carbon Nanotubes: A Quantitative Study of the Surface Properties of Biomimetic Nanofibrous Scaffolds. *ACS Nano* **2009**, *3*, 3200−3206.
(40) Fu, C.; Meng, L.; Lu, Q. "Hierarchical Self-Assembly" of Helical Amylose/SWNTS Complex. *Sci. China, Ser. B: Chem.* **2008**, *51*, 269−274.
(41) Bachilo, S. M.; Strano, M. S.; Kittrell, C.; Hauge, R. H.; Smalley, R. E.; Weisman, R. B. Structure-Assigned Optical Spectra of Single-Walled Carbon Nanotubes. *Science* **2002**, *298*, 2361−2366.

(42) Dresselhaus, M. S.; Dresselhaus, G.; Saito, R.; Jorio, A. Raman Spectroscopy of Carbon Nanotubes. *Phys. Rep. Rev. Sec. Phys. Lett.* **2005**, *409*, 47−99.
(43) Fu, C.; Meng, L.; Lu, Q.; Fei, Z.; Dyson, P. J. A Facile Strategy for Preparation of Fluorescent Swnt Complexes with High Quantum Yields Based on Ion Exchange. *Adv. Funct. Mater.* **2008**, *18*, 857−864.
(44) Zhu, W. H.; Minami, N.; Kazaoui, S.; Kim, Y. Fluorescent Chromophore Functionalized Single-Wall Carbon Nanotubes with Minimal Alteration to Their Characteristic One-Dimensional Electronic States. *J. Mater. Chem.* **2003**, *13*, 2196−2201.
(45) Taneja, P.; Ayyub, P.; Chandra, R. Size Dependence of the Optical Spectrum in Nanocrystalline Silver. *Phys. Rev. B* **2002**, *65*, No. 245412.
(46) Liz-Marzan, L. M.; Giersig, M.; Mulvaney, P. Synthesis of Nanosized Gold-Silica Core−Shell Particles. *Langmuir* **1996**, *12*, 4329−4335.
(47) Antaris, A. L.; Robinson, J. T.; Yaghi, O. K.; Hong, G.; Diao, S.; Luong, R.; Dai, H. Ultra-Low Doses of Chirality Sorted (6,5) Carbon Nanotubes for Simultaneous Tumor Imaging and Photothermal Therapy. *ACS Nano* **2013**, *7*, 3644−3652.